Preprint: *2001 AMOS Technical Conference, 10-14 September 2001, Maui, Hawaii*

AN OPTICAL SURVEY FOR SPACE DEBRIS IN THE GEOSTATIONARY RING

T. Schildknecht[(1)], R. Musci[(1)], M. Ploner[(1)], J. de Leon Cruz[(2)], L. de Fatima Dominguez Palmero[(2)]

[(1)] Astronomical Institute, University of Bern, Sidlerstrasse 5, CH-3012 Bern, Switzerland
Email: thomas.schildknecht@aiub.unibe.ch
Email: reto.musci@aiub.unibe.ch
Email: martin.ploner@aiub.unibe.ch

[(2)] Instituto de Astrofisica de Canarias, 38200 La Laguna, Tenerife, España
Email: jmlc@ot.iac.es
Email: ldp@ll.iac.es

ABSTRACT

It has been suspected since a long time that the geostationary ring (GEO ring) may contain a population of small debris objects. The current catalogue population, e.g. from the US Space Command catalogue, is, however, limited to objects larger than about 1 m^2. In view of this situation, several space agencies started to perform optical observations of the GEO ring under the auspices of the Inter-Agency Space Debris Coordination Committee (IADC). The European Space Agency (ESA) initiated its own program for optical observations of space debris using a 1 m Ritchey Chrétien telescope on Tenerife (Canary Islands).

After a first test survey of 13 nights in 1999 the ESA telescope is now routinely used for GEO surveys since January 2001. We describe the search strategies, the object detection and data reduction procedures of the surveys. After a brief analysis of the errors of the estimated orbital elements we present the main results from the ESA campaigns. The data clearly confirms the substantial population of small objects in the size range from 1 to 0.1 m which was first detected in the 1999 test survey. Furthermore, for the first time a clear signature of 'clouds' of faint objects has been seen which can be most easily explained by single sources or events.

1. INTRODUCTION

The Geostationary Earth Orbit (GEO) is one of the most valuable regions for telecommunication, Earth observation and space science. Knowing the current debris population in this region is crucial to understand its future evolution and to implement mitigation measures to preserve this environment. The GEO region is especially fragile due to the extremely long lifetimes of debris at this altitude.

Current catalogues and models show a much lower spatial density of small objects in the GEO region than in most Low Earth Orbit (LEO) altitudes. The limiting object size for the catalogues is about 1 m. For smaller objects we therefore must rely on models. The MASTER model predicts less than 100 fragments in the size range from 0.1 to 1 m [1]. This may be explained by the fact that only two explosions are known to have occurred in GEO (a breakup of an Ekran spacecraft in 1978 and an explosion of a Titan rocket upper stage in 1992). Given this very limited information we may ask if the models reflect the real GEO environment or rather the missing input from observations.

2. THE ESA SPACE DEBRIS TELESCOPE

The ESA Space Debris Telescope is installed in the Optical Ground Station (OGS) at the Teide Observatory on Tenerife, Canary Islands. The OGS serves for the in-orbit checkout of the optical communication payload of the Artemis spacecraft. The ESA Space Debris Telescope is a classical astronomical telescope with a 1 m primary mirror and an English mount. For the debris observations we use the modified Richey-Crétien focus which is equipped with a CCD camera. The focal plane array consists of a mosaic of four 2k x 2k pixel CCDs. The total field of view is about 0.7 x 0.7 square degrees and the pixel size is 0.6 arcseconds.

3. THE SURVEY TECHNIQUES

3.1. Where to search?

Due to the small field of view of 0.7 degrees it is almost prohibitive to perform a complete survey of the GEO region accessible from Tenerife. An incomplete sample, however, will always be compromized by some selection effect. These selection effects may be minimized (or may be corrected) by a careful choice of the survey fields—provided that some general properties of the sampled population are known. For debris objects in GEO the latter is simply not the case. One reasonable assumption would be that the catalogue population is roughly tracing the debris population. We therefore have a look at some specific characteristics of the catalogue population.

Due to gravitational perturbations the orbital planes of GEO objects have a very specific distribution. The orbital planes of uncontrolled objects exhibit precessional motions, which manifests themselves in periodic variations of the inclinations between 0 and 15 degrees with a period of about 53 years. These precessional motions also result in a correlation between the inclinations and the right ascensions of the ascending nodes. Figure 1 shows the apparent density of the catalogued GEO objects in the right ascension-declination-system, i.e. as seen in front of the stellar background. The small squares mark survey fields (see below), the dark ellipse indicates the Earth shadow on January 21, and the light band between 6 and 8 hours right ascension indicates the Milky Way region.

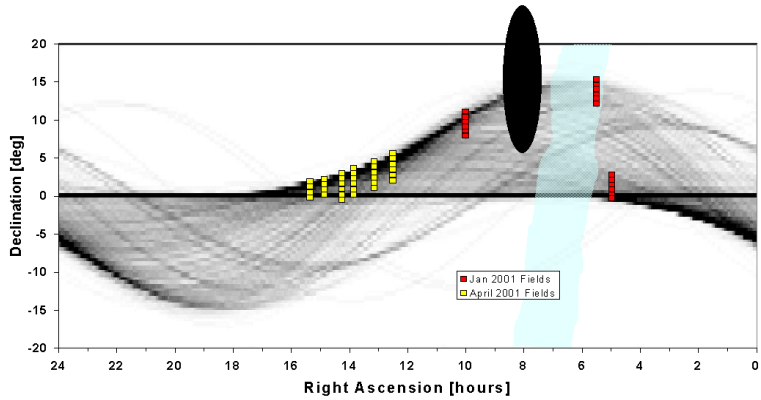

Figure 1. Apparent density of the catalogued GEO objects in the right ascension-declination-space. The small squares mark survey fields, the dark ellipse indicates the Earth shadow on January 21, and the light band between 6 and 8 hours right ascension indicates the Milky Way region.

3.2. Observations

The observation scenarios for the 2001 campaigns where chosen to optimize the coverage for certain bands of orbital inclinations while still considering observational constraints. With first priority we observed near the Earth's shadow cone in order to optimize the illumination conditions for the objects of interest. During January we had to avoid the Milky Way, which covered a good part of the evening sky just west of the shadow region. The search fields were furthermore placed at the densest region of the catalogue population. In order to increase the probability to re-observe the same objects during several consecutive nights, the same sequence of fields was imaged at the same local times during all the nights. Figure 1 shows the search fields for the January and the April 2001 campaigns in the right ascension-declination-system (the small squares roughly correspond to the field of view of the CCD camera.

The detection technique is based on an algorithm comparing several consecutive frames of the same field in the sky. Background stars are identified on a series of 10 to 30 frames, and the remaining parts of the frames are scanned for any additional objects. During the exposures the telescope is staring into an Earth fixed direction, i.e. is not tracking the stars but potential geostationary objects. After each exposure the telescope has to be repositioned so that the same area of the sky is passing the field of view at the next exposure. The frames are usually exposed for 2 seconds, which is a compromise between a high signal to noise ratio for the objects (long exposures) and a reasonable length for the star trails (short exposure). The exposure repetition rate for a particular field was set to one per minute meaning that any geosynchronous object detected would be visible on three consecutive frames. Given the current maximum frame repetition rate of about one per 30 seconds (including the repositioning of the telescope) we are able to observe two adjacent fields in parallel.

3.3. Data Reduction

All data was processed in quasi-real-time at the observatory (the results are available about 30 minutes after the observations). The processing is done in batches of about 30 consecutive frames of the same sky field.

The detection procedure is based on a 'masking technique'. The mask is generated from a median frame of the series and thus contains all objects that did not move during the entire series. It particularly contains all background stars. This mask is then applied to each individual frame and the unmasked parts are scanned for objects. A filter marks cosmic ray events by virtue of the shape of their intensity profile.

The objects detected at the level of single frames are then correlated and moving objects discriminated according to the expected minimum and maximum apparent motion. For all moving objects their astrometric positions on the individual frames are determined using catalogue stars as a reference. The accuracy of the positions of the objects depends on their magnitude and their apparent motion, but it is well below one arcsecond even for the faintest objects. Finally a circular orbit was determined for each object (the short arc spanning a few minutes only does not allow to estimate an eccentric orbit).

The correlation with a TLE reference catalogue is done by comparing the observed position with the predicted position as well as by comparing the orbital elements. We thus obtained a list of objects including the determined elements and the TLE data for the correlating objects and a set of small subframes for each detection. The subframes may be used later to manually screen the results. At this stage the uncorrelated ('unknown') objects are given a working name. A correlation of the unknown objects among the night or even among different nights must be done off-line only.

4. ERROR ANALYSIS FOR THE ORBITAL ELEMENTS OF KNOWN OBJECTS

In order to assess the accuracy of the estimated orbits we used TLEs from the US Space Command catalogue as a 'ground truth'. For this purpose we selected a set of 1303 measurements of known objects (i.e. which correlated with the TLE catalogue) from the January to April 2001 campaigns. All objects were detected in the course of regular surveys, i.e. under exactly the same conditions as the unknown objects. Their orbital elements were determined from two or three consecutive position observations, representing short arcs of about one to two minutes. Only circular orbits were determined (eccentricity assumed 0). The accuracy of the individual astrometric positions is better than 1 arcsecond.

Assuming no errors for the TLEs the comparison between the two sets of elements would directly yield the quality of our orbit determination. However, the TLEs are not error-free and the mentioned comparison will give 'worst case' figures for the quality of the determined orbits.

We would finally like to apply the results from this error analysis for unknown objects. There are two caveats: a) unknown objects are much fainter and their positions will be less accurate (by a factor of two), and b) the assumption of circular orbits may be not valid any more.

The mean values and standard deviations for the differences between the determined orbital elements and the corresponding TLEs are given in Table 1. The differences in semimajor axis, inclination, right ascension of ascending node, longitude, and latitude are indicated by Δa, Δi, $\Delta\Omega$, $\Delta long$, and Δlat respectively. The values for the ascending node have been compared for objects with inclinations larger than 2 degrees only.

Table 1. Mean values and standard deviations for the differences between the determined orbital elements and the corresponding TLEs from a set of 1303 observations.

$\overline{\Delta a}$	= 17.0	± 79.5	km
$\overline{\Delta i}$	= 0.01	± 0.05	deg
$\overline{\Delta\Omega}$	= 0.08	± 0.46	deg
$\overline{\Delta long}$	= 0.02	± 0.15	deg
$\overline{\Delta lat}$	= 0.002	± 0.02	deg

Taking into account the corresponding standard deviations, all values are compatible with the expectation value 0. The values for the differences in the semimajor axis, the inclination, and the right ascension of ascending node are most likely dominated by errors in the determined orbit. (Which in turn are determined by the accuracy of the astrometric positions and the short (!) arc of about one minute.) The differences in longitude and latitude, on the other hand, are directly reflecting the accuracy of the ephemerides generated from the TLEs (the position error of the

measurements is negligible). In order to illustrate that there is no systematic behavior of the errors we show the distribution of the differences for the inclination (Figure 2, left) and for the right ascension of the ascending node (Figure 2, right).

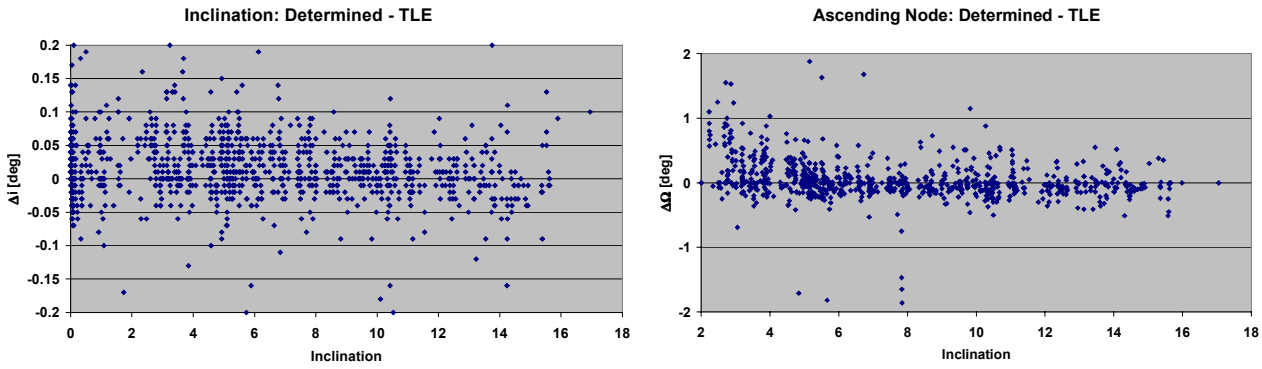

Figure 2. Differences between the determined inclination and the corresponding TLE (left) and between the determined ascending node and the corresponding TLE (right) for a set of 1303 observations.

5. RESULTS

Table 2 gives an overview of the ESA GEO campaigns until July 2001. The table includes the 1999 test campaign, which consisted in fact of a first, very limited series of system tests [2]. By 'unknown detections' we denote the detection of an uncatalogued object within a single 30-minute observation series. Some of these detections may actually refer to the same object, i.e. we may have incidentally re-observed some of the objects during the campaign. We use the term 'unknown objects' for uncatalogued objects after having correlated all detections from the campaign. This latter task is identical with the creation and maintenance of a temporary catalogue of orbital elements for the unknown objects. Currently only the data from the January 2001 through the April 2001 campaigns have been postprocessed.

Table 2. ESA GEO Campaigns

	Aug/Sept 1999	Jan – Apr 2001	Jan – Jul 2001
Frames	5'400	41'500	62'500
Scanned Area	895 deg^2	7390 deg^2	11200 deg^2
Obs. Time	13 nights / 49 h	51 nights / 346 h	82 nights / 521 h
Image Data	52 GB	330 GB	500 GB
Unknown detections		**926**	**?**
Unknown objects	**150**	**?**	**?**

Before presenting the results let us mention a caveat. When trying to learn something about the real environment we must be aware of the potentially strong selectional biases of the observation data. If the population of unknown objects is not homogeneously distributed, the result will depend on where we place the search fields. The January to April 2001 data contains two extreme subsets: the January campaign where we predominantly observed at high latitudes and the April campaign with the majority of the fields at low latitudes. Corresponding diagrams showing the January and the April search fields in the horizon system are given in Figure 3. The observation time for the different latitudes is indicated in Figure 4.

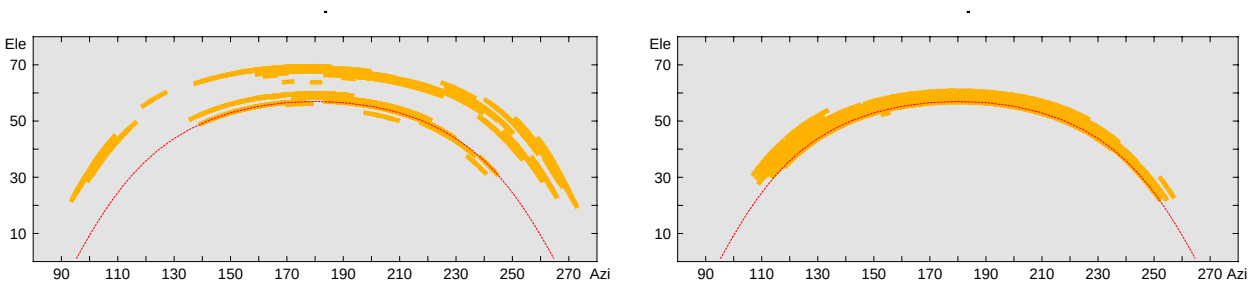

Figure 3. January (left) and April (right) 2001 search fields. The dotted line represents the celestial equator.

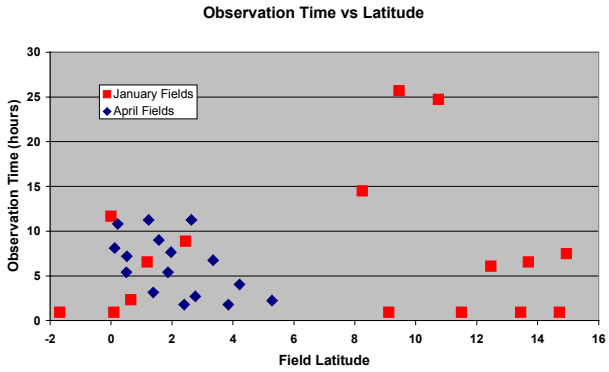

Figure 4. Observation time for different latitudes for the January and the April 2001 campaign.

5.1. Absolute Magnitude Distribution

Figure 5 shows the absolute magnitude distribution of all detections from the January to April 2001 campaigns. The solid line indicates the instrument sensitivity as determined from independent calibration measurements. All magnitudes have been reduced from apparent magnitudes to so-called absolute magnitudes by correcting for the illumination phase angle. For the scattering properties we assumed a simple Lambert sphere. No reduction to a common distance has been done because of the uncertainties of the determined orbits (see below). The value of this correction would be less than 0.5 magnitudes in most cases. The magnitudes are astronomical 'V magnitudes' and have an accuracy of a few 0.1 magnitudes except at the very faint end where errors could amount to 0.5 – 1 magnitude. The indicated object sizes were derived by assuming Lambert spheres and a bond albedo of 0.1. Both assumptions, however, are uncertain, as long as we don't know the nature of the observed objects.

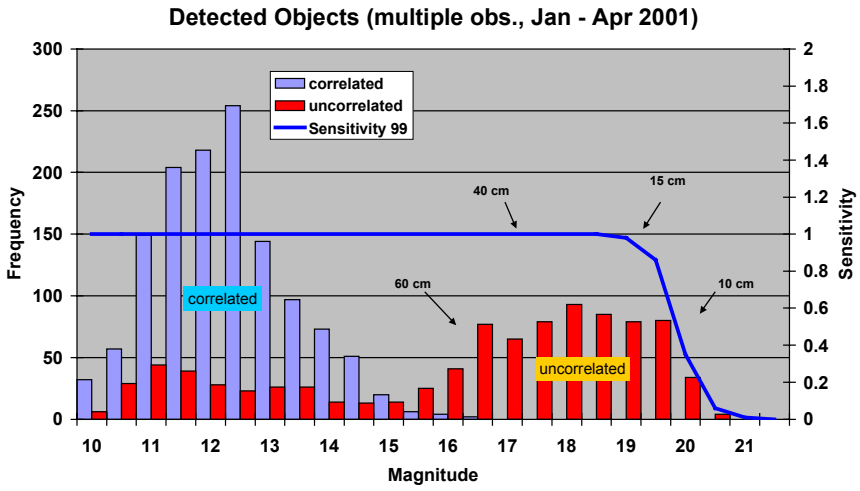

Figure 5. Absolute magnitude distribution for the detections of the January to April 2001 campaigns.

The distribution is bimodal with the correlated objects clustered around magnitude 12.5, and a large number of uncorreleated objects in the range from magnitude 15 to 21. It is important to note that the decrease in number of objects fainter than about magnitude 18 is entirely due to the sensitivity limit of the observation system. The real luminosity function beyond magnitude 18 could therefore still increase!

There are a considerable number of bright objects that did not correlate with the available catalogue. The majority of these objects are controlled objects at 0 degree inclination. In many cases the objects are members of groups of satellites co-located in the same 0.1-degree longitude slot. They did not firmly correlate with the catalogue due to the insufficient accuracy of the catalogue. In addition, classified objects were not contained in the reference catalogue.

We should refrain from directly comparing the number of uncorrelated with the number of correlated detections. Selection effects may crucially affect this ratio. This is obviously the case when comparing the results from the January campaign (Figure 6, left) with the results from the April campaign (Figure 6, right). The April survey, which was focused on the lower latitudes, yielded much less unknown detections than the January campaign, which was concentrating on higher latitudes (see also Figure 4). From this we may already suspect that there must be an excess of unknown objects at higher inclinations.

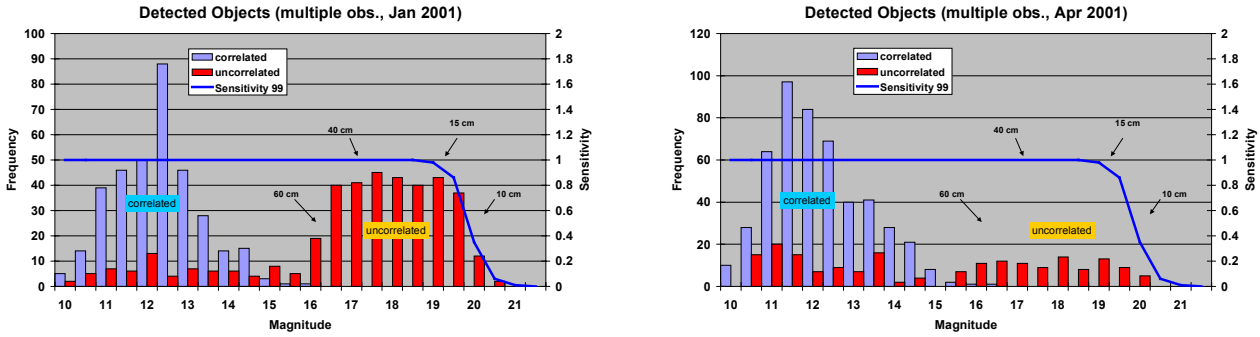

Figure 6. Absolute magnitude distribution for the detections of the January (left) and the April (right) 2001 campaign.

5.2. Orbit Inclination Distribution

The inclination distribution for the January to April campaigns is shown in Figure 7. The distribution of the uncorrelated detections differs significantly from the distribution of the correlated detections. There are clear excesses of uncorrelated detections around 13 and around 14 degree inclination.

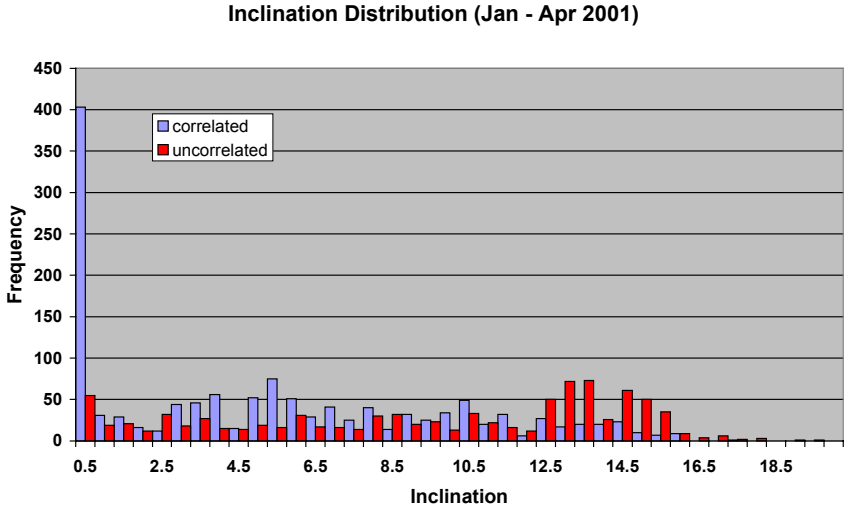

Figure 7. Inclination distribution for the detections of the January to April 2001 campaigns.

The effect is even more prominent in the January data set (Figure 8, left). During the April campaign, however, all search fields were located at low latitudes, preventing detection of a significant amount of high inclination objects (Figure 8, right).

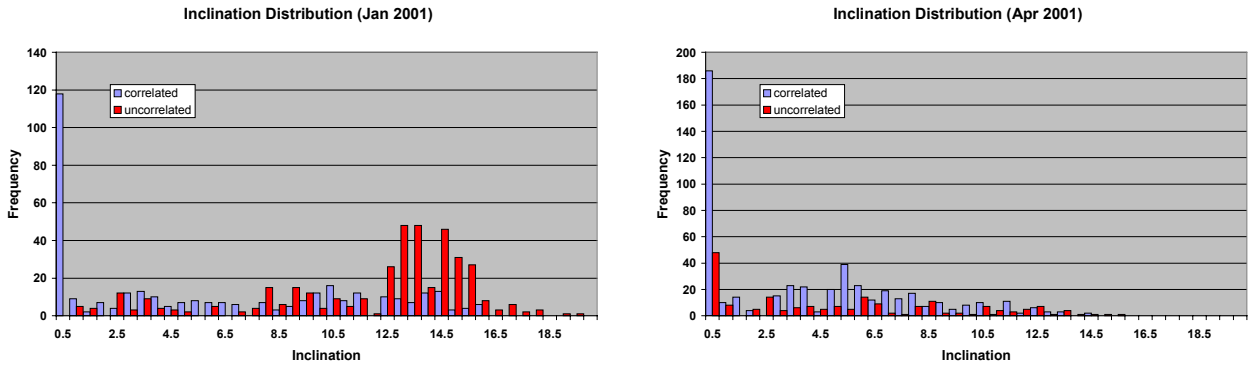

Figure 8. Inclination distribution for the detections of the January (left) and April (right) 2001 campaigns.

5.3. Distribution of Semimajor Axes

The distribution of the semimajor axes is given in Figure 9. The semimajor axes of the correlated detections are strongly concentrated around the nominal GEO altitude. On the other hand, the uncorrelated detections also have the peak of their inferred semimajor axes at GEO altitude but they are much more dispersed with a slight asymmetry. All semimajor axes were determined assuming circular orbits, which is certainly not true for all objects. In general, fixing the eccentricity at a wrong value may result in a large error of the inferred semimajor axis. The distribution given in Figure 9 may thus be—depending on the distribution of the true eccentricities—quite meaningless.

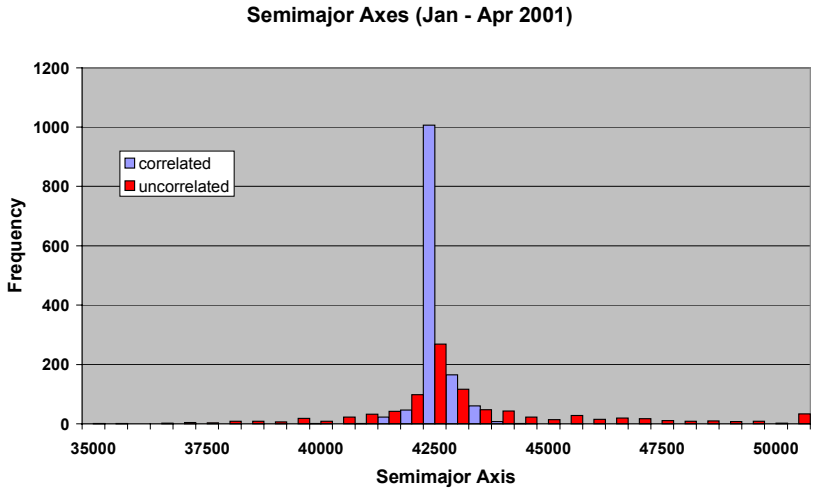

Figure 9. Semimajor axes of the detections of the January to April 2001 campaigns.

5.4. Orbit Inclination and Right Ascension of Ascending Node

The inclination and the right ascension of the ascending node are strongly correlated for the TLE population as we have seen in section 3.1. Figure 10 gives both elements for all correlated and uncorrelated detections. The distinct figure outlined by the correlated objects is due to the explained 53-year precession period of the orbital planes. Assuming that the objects started with orbits of 0 degree inclination the position in the diagram is indicating the time since the end of active inclination control. The orbits gradually evolve from low inclination and at right ascension of the ascending node of about 100 degrees to higher inclinations and lower right ascension of the node until they reach the maximum inclination of 15 degrees after 26.5 years. The oldest catalogue objects have passed this point already.

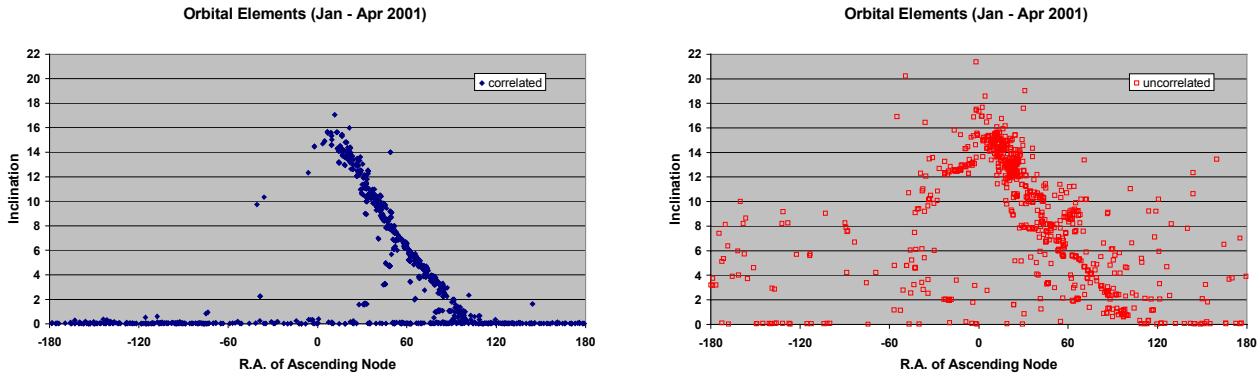

Figure 10. Inclination versus right ascension of ascending node for the correlated (left) and uncorrelated (right) detections of the January to April 2001 campaigns.

The uncorrelated detections seem to follow this general evolutionary pattern with a larger spread and include a 'background' component with a homogeneous distribution in the inclination-ascending node-space. But they also form some striking clusters. The groupings at 8, 9, 13, and 15 degrees inclination already showed an enhancement in the inclination distribution of the January survey. The fact that there are corresponding groupings in right ascension means that these objects in the clusters have common dynamical characteristics. We have checked the clusters for multiple sightings of the same objects and conclude that they are real (a pure selection effect can be excluded).

6. CONCLUSIONS

Current catalogues and models show a much lower spatial density of small objects in the GEO region than in most LEO altitudes. Only two explosions are known to have occurred in GEO. The limiting object size for the catalogues is about 1 m.

The results from the ESA GEO survey show a significant, hitherto unknown population of objects in the 0.1 to 1 m size range in the geostationary ring. The observed luminosity function is steadily rising towards smaller sizes up to the observational limit of about 15 cm.

A clear signature of 'clouds' of faint objects has been found. The only plausible source for this debris is break-ups of spacecraft, apogee boost motors and rocket upper stages. Due to the small field of view of the ESA telescope the survey is still inhomogeneous and observational selection effects must be carefully taken into account when using the data to improve debris models.

7. ACKNOWLEDGEMENTS

This work was done under ESA/ESOC contract 11914/96/D/IM. We thank Jyri Kuusela (ESOC) for the technical on-site support at OGS.

8. REFERENCES

1. Bendisch J., Bunte K. D., Krag H., Sdunnus H., Walker R., Wegener P., Wiedemann C., *"Upgrade of the ESA MASTER Model"*, Final report 12318/97/D/IM, Braunschweig, Germany, May 2000.
2. Schildknecht T., Ploner M. and Hugentobler U., *The Search for Debris in GEO,* 33rd COSPAR Scientific Assembly, July 16 – 23, 2000, Warsaw, Poland, to be published in Advances in Space Research.
3. Schildknecht T., Musci R., Ploner M., Preisig S., de Leon Cruz J., and Krag H., *Optical Observation of Space Debris in the Geostationary Ring,* 3rd European Conference on Space Debris, 19 – 21 March 2001, ESOC, Darmstadt, Germany.